Tevatron optics measurements and optics correction performed at August 22 and 29 of 2003

1. Optics measurements and corrections

The study performed on August 22 was devoted to on-line optics measurements with consequent optics corrections. Optics correction was applied in three iterations. Table 1 summarizes the results. As one can see from the table a very good match was achieved at the second iteration. It is verified by almost equal tune shifts for quads located at two different betatron phases (for each plane) and by measurements of Courant-Snyder invariants (see Table 1 and Figure 1).

The study performed on August 29 was devoted to minimization of emittance growth for the round trip MI-Tevatron-MI transfers. The results are presented in Table 2. Comparing Tables 1 and 2 one can see that the same optics corrections yield the tune shift and, consequently, the beta-functions at the measurement quads, which are different by 4% and 2%, correspondingly, for horizontal and vertical degrees of freedom.

Table 1. Results of optics measurements and optics corrections performed at August 22

		Initial	1st iter(delta)	2nd iter	3rd iter
Optics corrections	C:CQ9 [A]	63.92	45.9(-18)	63.92(0)	60.31
	C:CQ7 [A]	98.07	125.1(27)	98.07(0)	103.40
	C:DQ7 [A]	99.65	117.6(18)	108.65(9)	108.65
	C:DQ9 [A]	89.65	64.6(-25)	76.79(-12.86)	76.79
	T:SQ [A]	-2.827	-3.023	-2.852(-.025)	-2.852
	T:SQA0 [A]	4.185	6.680	4.361(0.176)	4.361
	QY(set)	20.568	20.551	20.55514	20.603
	QX(set)	20.605	20.58315	20.6096	20.55633
Measured tunes	QY(meas)	.575	.5752	.5756	.5752
	QX(meas)	.583	.5831	.5831	.5831
Optics meas. by 10 A quad current change, ΔQx/ΔQy	QE17	.0213/-.0075	.0249/-.0061	.0208/-.0071	.0214/-.0065
	QE19	.0207/-.0076	.0187/-.0080	.0208/-.0067	.0206/-.0076
	QE47	.0065/-.0255	.0068/-.0310	.0061/-.0287	.0061/-.0279
	QF33	.0059/-.0310	.0072/-.0239	.0059/-.0275	.0060/-.0266
ΔQx/ΔQy for ΔI=10 A predicted by model*	QE17			.0225/-.0077	
	QE19			.0210/-.0079	
	QE47			.0070/-.0287	
	QF33			.0069/-.0290	
Optics meas. with C.-S. invariants	Ax1	0.75	0.72	0.76	0.73
	Ax2	0.77 (+0.02)	0.79	0.77 (+0.01)	0.76
	Ay1	0.73	0.80	0.74	0.73
	Ay2	0.79 (+0.06)	0.74	0.77 (+0.03)	0.77

* The model uses periodic beta-functions in E and F sectors with coupling taken into account

Figures 2 and 3 present differential orbits and their fit for the corrected optics (2nd iteration in Table 1). Figures 3 and 4 present corresponding beta-functions and dispersions. The last four lines in Table 2 present the tune shifts computed with the model. One can see that the model predicts the horizontal and vertical tune-shifts at the central orbit with accuracy of 6% and 13% correspondingly. Predictions for pbar helix are significantly worse. They are 16% and 36% for horizontal and vertical tune-shifts, correspondingly. Comparing the measured tune shifts at the

central orbit and pbar helix one can also see that the horizontal and vertical tune-shifts are changed by 17% and 5% correspondingly. That is significantly less than the model predictions: 24% and 13%. The model also yields sufficiently large errors in chromaticities predictions (~16 units in each plane). That stresses that there are significant errors in the description of lattice nonlinearities. Presently, the only nonlinearities the model uses are the uniform sextupole component in all dipoles and all non-linear Tevatron correctors. That is oversimplification and needs to be corrected in the future.

Although there is some difference in optics for measurements performed at August 22 and 29 both measurements were used to build the model. Tables 3 and 4 present global and local optics corrections used in the model. As one can see from Figures 2 and 3 the model describes differential orbits with good accuracy but some improvements are still required to describe the dispersions. The dispersions are much more sensitive to focusing errors than the differential orbits excited by dipole correctors.

Table 2. Results of optics measurements and optics corrections performed at August 29

		Initial	Corrected optics (Delta)	Tune shift at pbar helix for corrected optics
Optics corrections	C:CQ9 [A]	63.92	63.92	
	C:CQ7 [A]	98.07	98.07	
	C:DQ7 [A]	99.65	108.65(9)	
	C:DQ9 [A]	89.65	76.79(-12.86)	
	T:SQ [A]	-2.805	-2.805	
	T:SQA0 [A]	3.705	3.705	
	QX(set)	20.609	20.606	
	QY(set)	20.551	20.551	
Measured tunes	QX(meas)	.582	.5825	.5831
	QY(meas)	.575	.5758	.5739
Optics meas. by 10 A quad current change, ΔQx/ΔQy	QE17 (X)		.0202/-.0066	.0236/-.0073
	QE19 (X)		.0217/-.0079	.0204/-.0042
	QE47 (Y)		.0063/-.0283	.0055/-.0298
	QF33 (Y)		.0055/-.0270	.0050/-.0265
ΔQx/ΔQy for ΔI=10 A predicted by model*	QE17 (X)		.0211/-.0084	.0262/-.0083
	QE19 (X)		.0230/-.0067	.0238/-.0054
	QE47 (Y)		.0064/-.0299	.0057/-.0284
	QF33 (Y)		.0065/-.0310	.0074/-.0351

* The model was built using differential orbit measurements presented in Figures 1 and 2.

Table 3. Global optics corrections

Correction of dipole edge focusing	0.057 units* (0.039 deg of edge focusing per edge)
Skew-quadrupole field in the dipoles	1.36 units*
Sextupole strength in the dipoles	-3.2 units*
Focusing strength correction for main bus quads	+0.177%

* One unit represents 10^{-4} correction of dipole field at 1 inch radius.

Table 4. Point optics corrections

Corrections for the regular quads*		Corrections for the final focus quads	
Name**	Value, kG	Name	value
A11s	3.5	F_B0Q3	0.6%
A13	1	Roll_B0Q3D	-0.05 deg
A15	4	Roll_B0Q3F	-0.02 deg
A17	-3	F_D0Q3	0.7%
A28	-2		
A32	1		
A34	2		
A42s	-4		
A42	-2		
A44	1		
A46	1		
A46s	-3		
B15	-1		
B15s	-2		
B17s	-2		
B23	2		
B28	-1		
B38s	1		
B42	1		
B42s	-2		
B44	5		
C13	1		
C13s	5		
C17	-2		
C17s	-1		
C45	2		
C46s	1		
D16s	-5		
D45	4		

* The integral strength of regular Tevatron quad at injection is 191.2 kG

** Character “s” at the name end denotes skew-quads

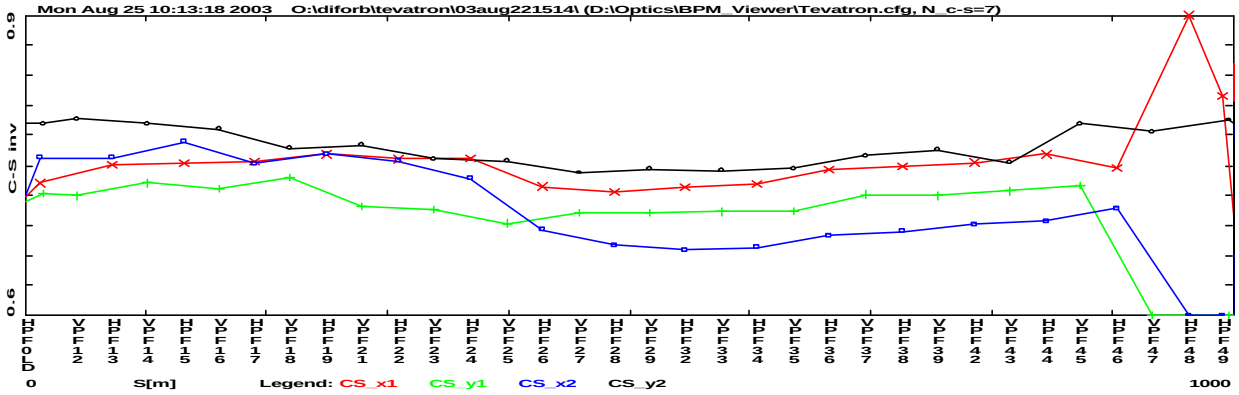

Reference

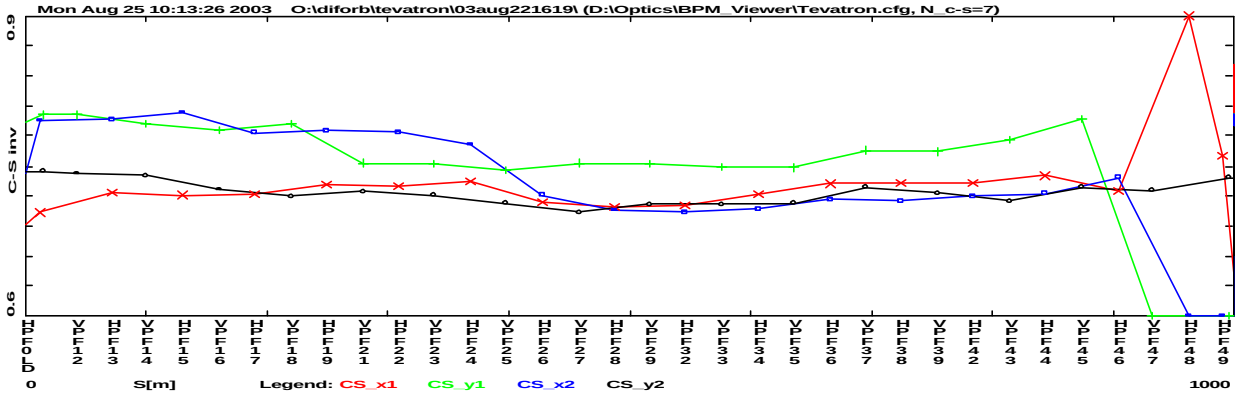

First iteration

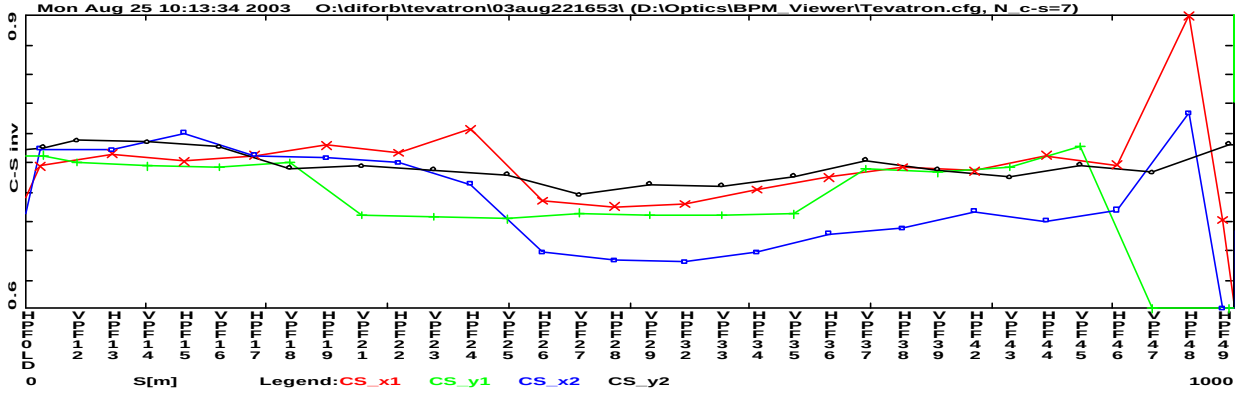

Second iteration

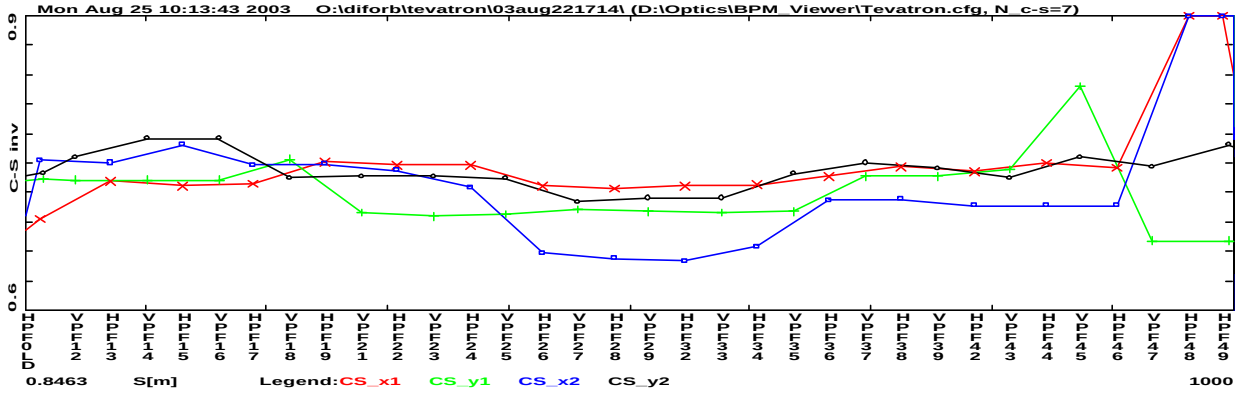

Third iteration

Figure 1. Courant-Snyder invariants in vicinity of injection point for different steps in optics correction

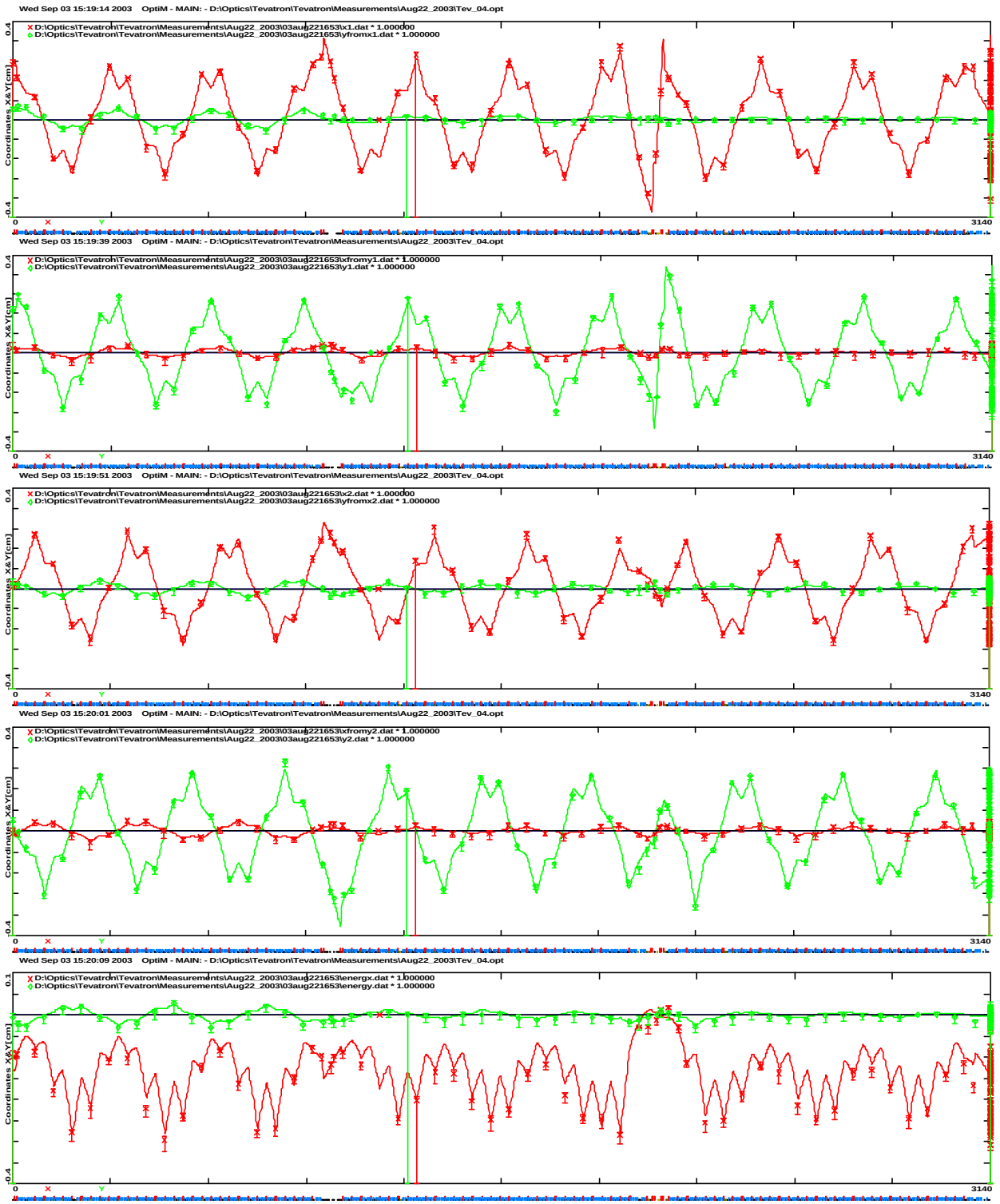

Figure 2. Differential orbits for the first Tevatron half after Tevatron optics correction

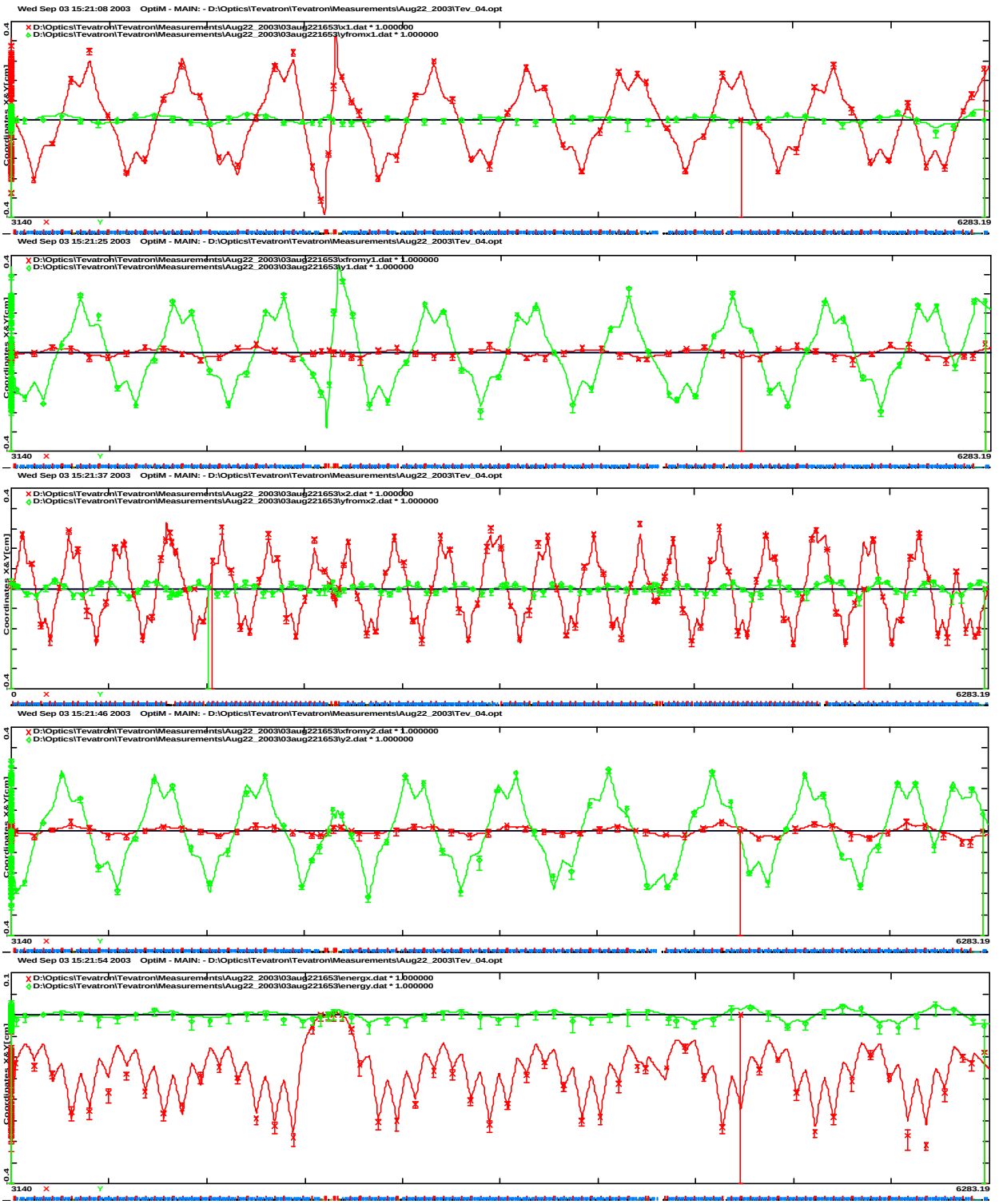

Figure 3. Differential orbits for the second Tevatron half after Tevatron optics correction

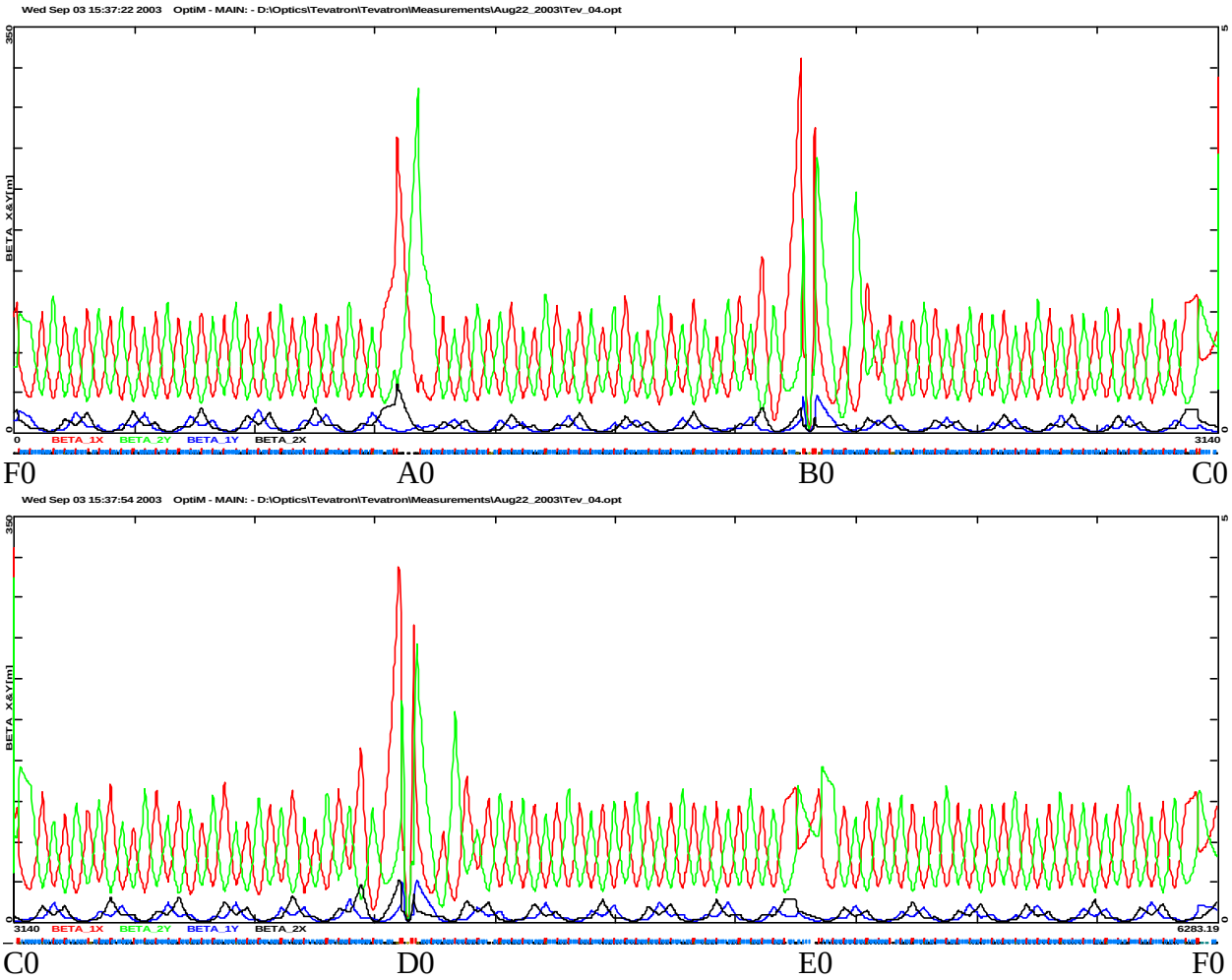

Figure 4. Beta-functions restored from differential orbit measurements for central orbit

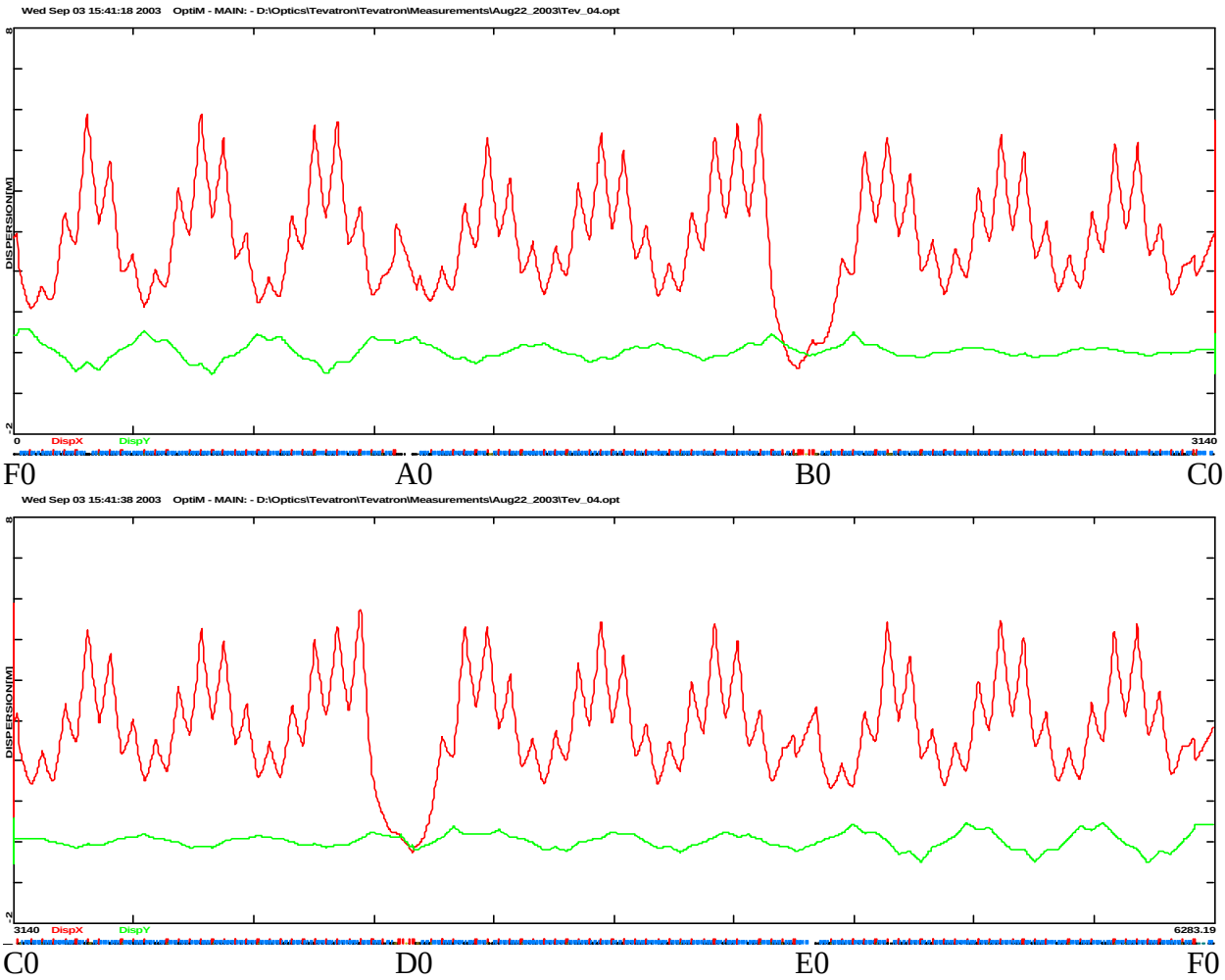

Figure 5. Dispersions restored from differential orbit measurements for central orbit

2. Measurements and predictions of the round trip emittance measurements MI-Tevatron-MI

Table 5 and Figure 6 present measured and computed round trip emittance growths for uncorrected and corrected Tevatron optics. One can see that both the computations and the measurements verify that the Tevatron optics correction makes little effect on the emittance growth. Computations are carried out for the Tevatron beta-functions presented in Table 6. They take into account that the transfers to Tevatron go to the central orbit, and the transfers to MI go from pbar helix. We also presume that the both transfer lines are perfectly matched to the design Tevatron lattice, and both emittances are initially equal. Computations yield that due to coupling each of two transfers yields about ~12.5% emittance growth in each plane, while the measured beam envelope mismatch contributes much smaller value, ~1-1.5%. Moreover the model even predicts a small increase of the emittance growth for better-matched Tevatron lattice. This is related to the fact that the real non-linearities of Tevatron magnets are not included in the model. Therefore the model does not describe coupling on the pbar helix sufficiently well, and, consequently, the errors in coupling description contribute more to the emittance decrease than the optics mismatch to the emittance increase. In contrast, if the proton extraction goes from the central orbit the computations yield ~1% improvement per transfer for the corrected Tevatron lattice.

As one can see in Figure 6 the accuracy of vertical emittance measurements in MI is much worse than horizontal ones. It is related to the malfunctioning of vertical emittance monitor. Rms accuracy of emittance monitors is: 0.6 mm mrad and 3 mm mrad, correspondingly, for horizontal and vertical monitors.

Taking into account good agreement between predicted and measured emittances and that the computations predict the same emittance growth for both transfers we believe that beam emittance in Tevatron is the average of incoming and outcoming MI emittances. The horizontal emittance measurements in Tevatron are 0.7 mm mrad above the "average" MI emittance which is within the measurement accuracy. The vertical Tevatron emittance is 4 mm mrad above the MI averaged emittance. That is not only well outside the measurement accuracy but is well above (by 2.6 mm mrad) the emittance of the beam returned to MI. The reason of this discrepancy is not understood. Note also that the vertical emittance growth during shots includes this error and therefore is strongly overestimated.

Table 5. Measured and computed* round trip emittance growth

	Uncorrected (old) Tevatron optics		Corrected (old) Tevatron optics	
	Measured	Computed	Measured	Computed
$\delta\varepsilon_x$ [mm, mrad]	4.22±0.21	2.54	4.07±0.12	3.08
$\delta\varepsilon_y$ [mm, mrad]	1.58±1.47	3.40	2.83±0.61	2.98
$(\delta\varepsilon_x + \delta\varepsilon_y)/2$, [mm, mrad]	2.9	2.97	3.45	3.03

* Computations were carried out for equal horizontal and vertical emittances of 11 mm mrad.

Presently, Tevatron dipoles are the main source of coupling between vertical and horizontal planes. To reduce coupling we are going to correct skew-quadrupole terms for Tevatron dipoles, which do not have nearby skew-quadrupole correctors. There are 106 Tevatron dipoles to be shimmed. They are located in A44-B19 and C44-D19 regions. That should reduce the emittance growth from about 13% per transfer to about 3%. Figures 7 and 8 present the projections of betatron modes into XY plane and the auxiliary beta-functions of Ripken parameterization (the

projections of beta-functions to another plane) for the case of optimal machine decoupling with all available skew-quad families. One can see that the suggested correction of skew-quadrupole in dipoles allows significantly reduce coupling.

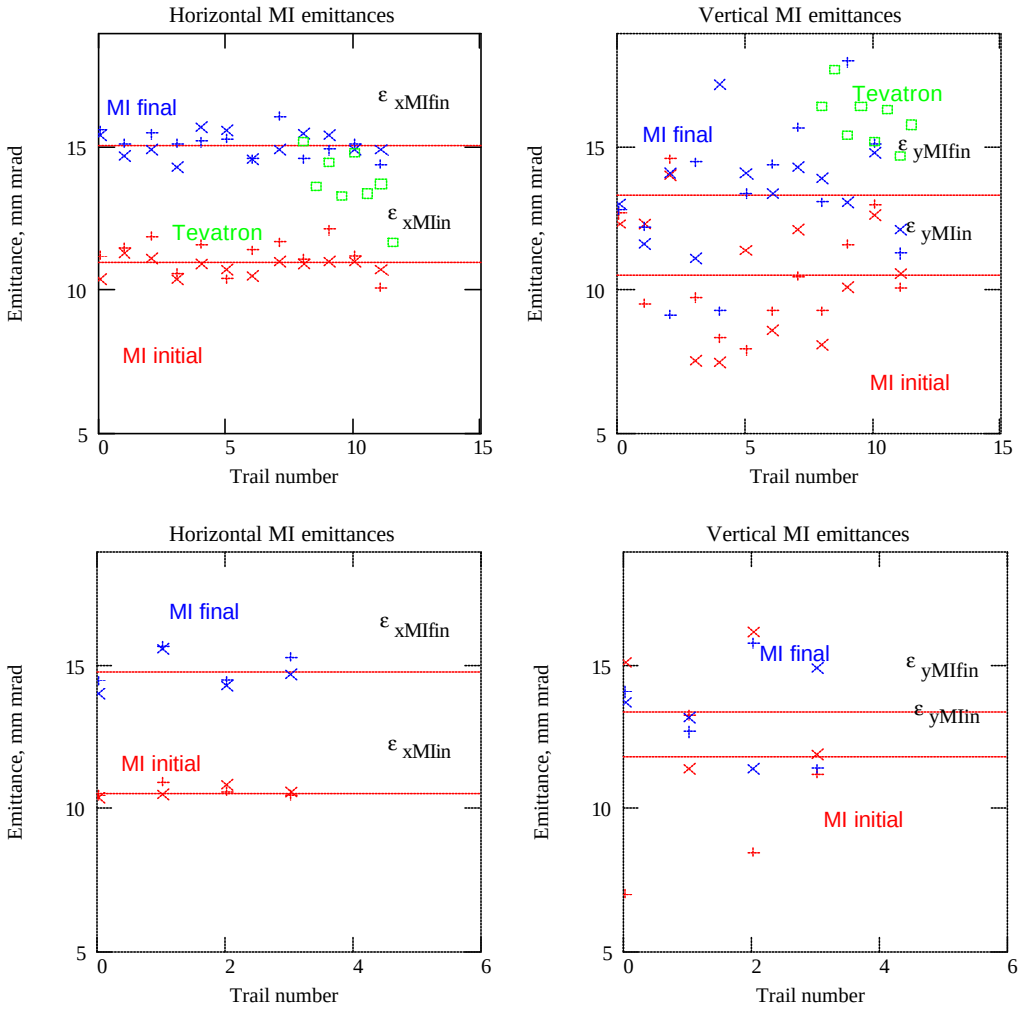

Figure 6. Measured emittances in MI before extraction to Tevatron (red) and for the beam coming back from Tevatron (blue), and in Tevatron (green); x – first fly data, + - second fly data.

Table 6. Twiss parameters for proton and pbar injection computed from the model

	Central orbit, proton injection point		P-bar helix, pbar injection point	
	Mode 1 (X)	Mode 2 (Y)	Mode 1 (X)	Mode 2 (Y)
b_x	9989.06	1641.6	7723.07	957.12
a_x	-0.825584	-0.199957	-0.65212	-0.14693
b_y	1066.57	5660.58	720.225	6491.63
a_y	0.0378417	0.160498	-0.060895	0.568122
ν	-110.965	-90.8895	-0.227463	-0.386324
u	-0.0276832		.0149636	
D_x	280.854		251.107	
$D\ell_x$	0.0175981		0.013067	
D_y	42.0776		8.9108	
$D\ell_y$	0.000276155		0.00107782	

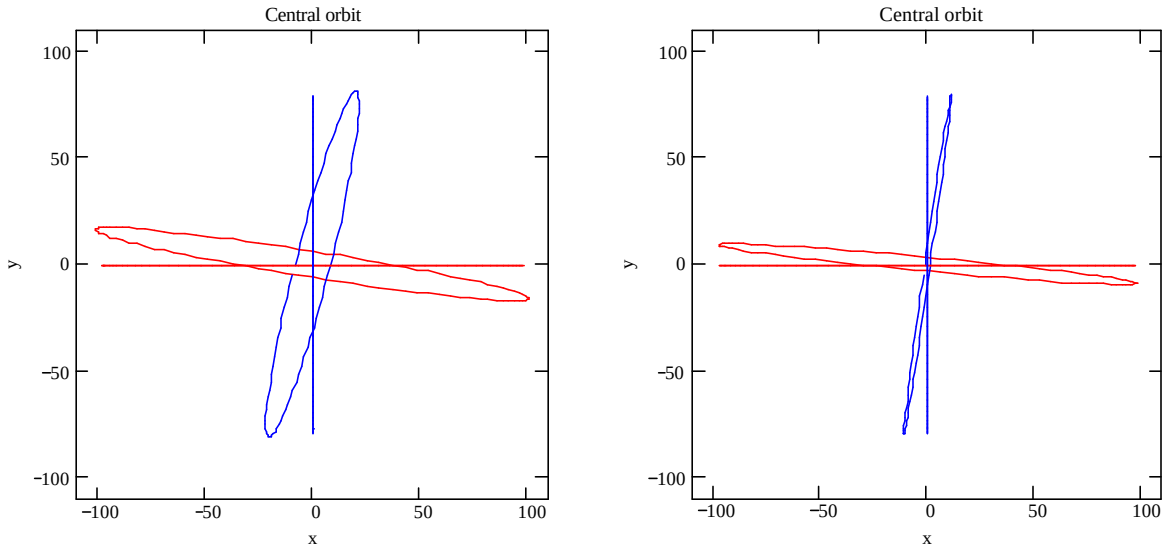

Figure 7. Projections of betatron modes to X-Y plan at proton injection point for present Tevatron (left) and after correction of skew-quadrupole component.

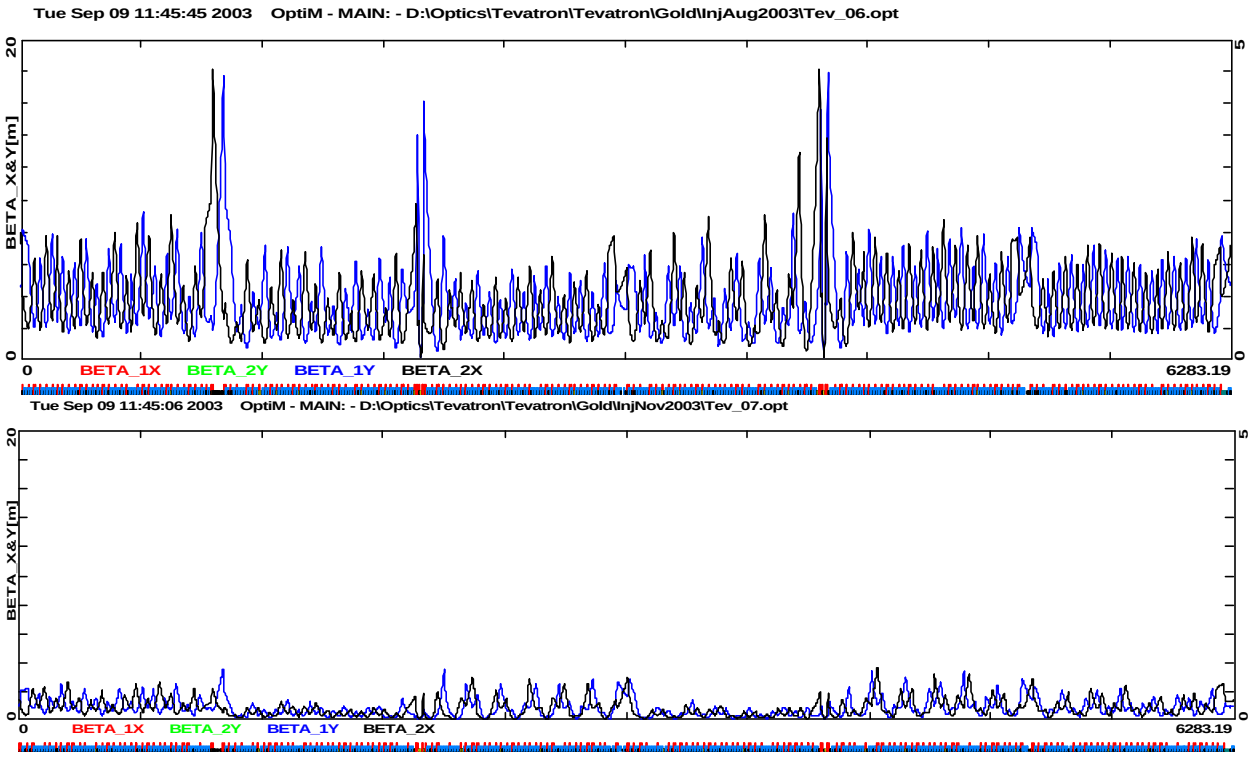

Figure 8. Projections of betatron functions to orthogonal plan for present Tevatron (top) and after correction of skew-quadrupole component (bottom).